Modeling and Investigation of Small-Signal Stability of DFIG-based Wind Energy System using Linear Quadratic Integral Controller

Ravi Bhushan
Student Member, IEEE
Department of Electrical Engg.
Indian Institute of Technology
(Indian School of Mines),
Dhanbad, India
ravibhushaniitbhu@gmail.com

Kalyan Chatterjee
Department of Electrical Engg.
Indian School of Technology
(Indian School of Mines),
Dhanbad, India
kalyanbit@yahoo.co.in

***Abstract*— This work demonstrates the effectiveness of the linear quadratic integral (LQI) controller over the linear quadratic regulator (LQR) controller for the small-signal stability of the doubly fed induction generator (DFIG)-based wind energy system. To design the proposed controller, the studied system has been described by the state-space linearization methodology. The eigenvalues and time response analysis method are used to examine the small-signal stability as well as the dynamic responses of the system. This study also considers to cancel the steady-state offset values in the powers flow through the DFIG and the generator-angular speed for complete disturbance rejection during the mechanical torque variations which are caused by the change in the wind speed. All the simulation results are performed in the MATLAB/SIMULINK and conclude that the proposed controller is much better than the classical LQR controller in terms of damping, eigenvalues, peak values and steady-state errors in the output variables.**

Keywords*— doubly fed induction generator; eigenvalues; small-signal stability; linear quadratic regulator; linear quadratic integral

I. Introduction

Since nowadays renewable power penetration continually increases and among all forms of renewable power, wind power is the most extensively and effectively used worldwide. Therefore, the modeling and stability of DFIG system are the essential concern of wind power generation. The stochastic and a non-linear nature of the wind speed also raise the various challenges in the design and control of the DFIG system. Recently, DFIG has been the most preferred wind turbines because it has a capability of varying speed, delivers 10-15% greater energy capture from the wind, small investment and the flexible control [1], [2]. The stator coil winding of the DFIG generally directly linked to the grid and its rotor winding is fed back through AC-DC-AC converter [1], [3]. In this paper, the high switching dynamics of the converter have been ignored.

In papers [4]–[12], the modeling and the small-signal stability of the DFIG system operates by PI controllers, which provide adequate performance in normal grid circumstances, but it may not be guaranteed especially under large perturbations. PI controllers are very effective in the first order single-input-single-output (SISO) model of the DFIG, but facing complications in dynamic analysis of the multi-input-multi-output (MIMO) system. Therefore, the concepts of non-linear robust controllers such as H-infinity [13], Linear Quadratic Gaussian (LQG) [14] or LQR [15]–[20] are utilized to overcome these problems.

In the modern optimal control scheme, the LQR is the well-known method which is related to the state-space representation and therefore suitable for the MIMO systems. The LQR has a property to regulate optimally the states and its output to zero, but it may face the problems with reference tracking or disturbance rejection, which is the desire in practice. Therefore, an integrator has been added in series with the studied system to track the desired output or reject the disturbance signal. This Linear Quadratic Integral (proposed) controller assures the zero steady-state error as well as enhancing the dynamic performance of the DFIG-based wind energy system [21]–[24].

For the small-signal stability study, the eigenvalue analysis technique has been used, which provides the inherent dynamic features of the studied system. The comparative simulation analysis between (i) LQR and (ii) LQI controller have been carried out in this study.

The structure of this study is systematized as follows; section II exhibits the mathematical modeling and the small-signal stability concept of the DFIG system. The control techniques for the DFIG are elaborated in section III. In section IV, the detailed analysis of simulation results and its discussion are explored and conclude the paper in section V.

II. Modeling and Small-Signal Stability Study of the DFIG System

The DFIG-based wind energy system deliberated in this work is represented in Fig. 1.

978-1-4799-5141-3/14/$31.00 ©2016 IEEE

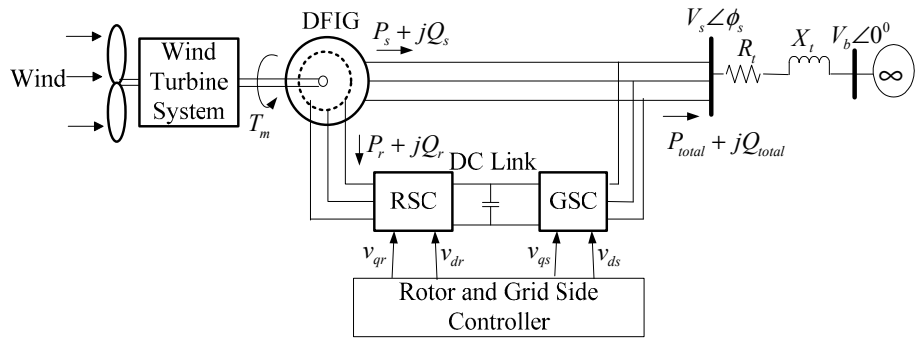

Fig. 1: Grid-connected DFIG system

In this section, the complete mathematical modeling and the small-signal stability concepts have been discussed with the help of DFIG basic equations as follows [7], [12]:

A. Modeling

$$\psi_{ds} = L_{ss} i_{ds} + L_m i_{dr} \tag{1}$$

$$\psi_{qs} = L_{ss} i_{qs} + L_m i_{qr} \tag{2}$$

$$\psi_{dr} = L_m i_{ds} + L_{rr} i_{dr} \tag{3}$$

$$\psi_{qr} = L_m i_{qs} + L_{rr} i_{qr} \tag{4}$$

$$v_{ds} = -R_s i_{ds} - \omega_s \psi_{qs} - \frac{1}{\omega_B} p(\psi_{ds}) \tag{5}$$

$$v_{qs} = -R_s i_{qs} + \omega_s \psi_{ds} - \frac{1}{\omega_B} p(\psi_{qs}) \tag{6}$$

$$v_{dr} = -R_r i_{dr} - (\omega_s - \omega_r)\psi_{qr} - \frac{1}{\omega_B} p(\psi_{dr}) \tag{7}$$

$$v_{qr} = -R_r i_{qr} + (\omega_s - \omega_r)\psi_{dr} - \frac{1}{\omega_B} p(\psi_{qr}) \tag{8}$$

$$L_{ss} = L_s + L_m \tag{9}$$

$$L_{rr} = L_r + L_m \tag{10}$$

Where, $p = \frac{d}{dt}$; (ψ_{qs}, ψ_{ds}) and (ψ_{qr}, ψ_{dr}) respectively represent the d-q axes stator and rotor flux linkages; (i_{qs}, i_{ds}) and (i_{qr}, i_{dr}) respectively represent the d-q axes stator and rotor currents; (v_{qs}, v_{ds}) and (v_{qr}, v_{dr}) respectively represent the d-q axes stator terminal and rotor voltages; $L_{ss} = 4.04pu$ and $L_{rr} = 4.0602pu$ respectively represent the stator and rotor self-inductance; $R_s = 0.005pu$ represents the stator resistance; $L_s = 0.04u$ represents the stator leakage inductance; $R_r = 0.0055pu$ represents the rotor resistance; $L_r = 0.0602pu$ represents the rotor leakage inductance; $L_m = 4.0pu$ represents the mutual inductance; $\omega_s = 1pu$ and ω_r respectively represent the synchronous and generator-angular speed; $(\omega_B = 2\pi f)$ represents the base speed; $f = 50Hz$ represents the nominal frequency.

The swing equation of single-mass model for wind turbine can be expressed as [7]:

$$p(\omega_r) = \frac{1}{2H} T_m - \frac{1}{2H} T_e \tag{11}$$

Where H is the total equivalent inertia of the system; T_m represents the mechanical torque and $T_e = (L_m i_{qs} i_{dr} - L_m i_{ds} i_{qr})$ represents the electromagnetic torque.

The powers flow through the DFIG can be evaluated as:

$$\left.\begin{aligned} P_s &= [v_{qs} i_{qs} + v_{ds} i_{ds}] \\ Q_s &= [v_{ds} i_{qs} - v_{qs} i_{ds}] \\ P_r &= [v_{qr} i_{qr} + v_{dr} i_{dr}] \\ Q_r &= [v_{dr} i_{qr} - v_{qr} i_{dr}] \end{aligned}\right\} \tag{12}$$

In this work, the DC-link capacitor dynamics is ignored by assuming grid-side converter control adequately fast such that the DC-link voltage remains unchanged and therefore, there is no reactive power exchange between the grid-side converter and the stator [6]. The reactive power supplied to the grid derives only from the stator side.

B. Small-Signal Stability Concept

This concept is one of the dominant approaches to linearize and knowing the inherent dynamic characteristics of the power system through eigenvalue analysis. The general linearized model is defined by the following state-space equations as [9], [15], [20]:

$$\dot{\Delta x} = A\Delta x + B\Delta u \tag{13}$$

$$\Delta y = C\Delta x + D\Delta u \tag{14}$$

Where, A, B, C, and D respectively represent the system state, input, output, and feed forward matrix. Δ denotes the small deviation and corresponding deviations in the state, input and output vectors are as follows:

$$\Delta x = \left[\Delta i_{qs}; \Delta i_{ds}; \Delta i_{qr}; \Delta i_{dr}; \Delta\omega_r\right] \tag{15}$$

$$\Delta u = \left[\Delta v_{qr}; \Delta v_{dr}; \Delta v_{qs}; \Delta v_{ds}; \Delta T_m\right] \tag{16}$$

$$\Delta y = [\Delta P_s; \Delta Q_s; \Delta P_r; \Delta Q_r; \Delta\omega_r] \tag{17}$$

III. Controllers for DFIG

In this study, all the state and output variables of the system are available for the feedback. Thus, the full state feedback LQR and the proposed LQI controller concept have been utilized to regulate the deviation in the stator and rotor active-

reactive power flow through the DFIG and in the generator-angular speed due to the variations in the mechanical torque or the wind speed to zero.

A. LQR Control Method

The structure of LQR control method is illustrated in Fig. 2. This technique minimizes the performance index *J*. The linear optimum control law $\Delta u = -K_{lqr}\Delta x$ has been chosen for performance index in the form of [15], [20].

$$J = \int_0^\infty \left(\Delta x^T Q \Delta x + \Delta u^T R \Delta u\right) dt \tag{18}$$

Here, *Q(5×5)* represents a real positive semi-definite matrix and *R(5×5)* represents a positive-definite matrix. $K_{lqr} = R^{-1}B'P$ is the optimal state-feedback gain matrix, which is calculated with the help of Riccati equation as [15], [20]:

$$A'P + PA - PBR^{-1}B'P + Q = 0 \tag{19}$$

Here, *P* represents a positive-definite matrix and values of the LQR weighting matrices are considered as:

$$Q_{lqr} = eye(5) \tag{20}$$

$$R_{lqr} = eye(5) \tag{21}$$

When (*A*, *B*) and (*Q*, *A*) respectively should be controllable and observable, then the closed-loop system $A_{lqr} = A - BK_{lqr}$ will be asymptotically stable.

In this case, the deviations in the output variables are not regulated to zero. Therefore, an integral controller has been added in the feedback path from the output variables (i.e. LQI controller) to reject any disturbances occur in the outputs of the DFIG system.

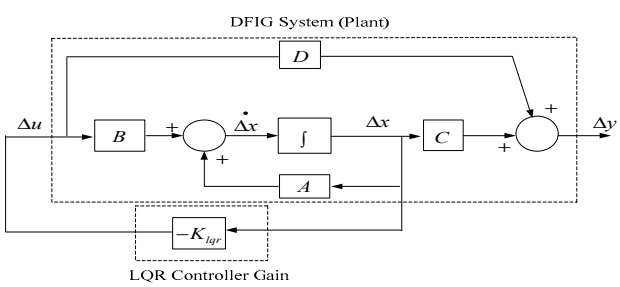

Fig. 2: Block diagram of LQR control scheme

B. LQI Control Method

The structure of LQI scheme is depicted in Fig. 3. In this control method, the control law depends on the both states Δx as well as the integral errors $\Delta e = [\Delta e_1; \Delta e_2; \Delta e_3; \Delta e_4; \Delta e_5]$ of the desired and the measured output as:

$$\Delta u_{new} = -K_{lqi}\Delta x_{new} = -\begin{bmatrix} K_x & K_y \end{bmatrix}\begin{bmatrix} \Delta x \\ \Delta e \end{bmatrix} \tag{22}$$

Where, $K_{lqi} = \begin{bmatrix} K_x & K_y \end{bmatrix}$ and $\Delta x_{new} = \begin{bmatrix} \Delta x \\ \Delta e \end{bmatrix}$ such that the main input of the studied system must be unaffected (i.e., $\Delta u = \Delta u_{new} + \Delta w$). Also

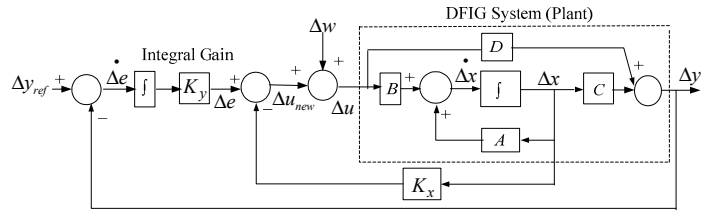

Fig. 3: Block diagram of LQI control scheme

$$\dot{\Delta x} = A\Delta x + B\left(\Delta u_{new} + \Delta w\right) \tag{23}$$

$$\dot{\Delta e} = -\Delta y + \Delta y_{ref} \tag{24}$$

$$\Delta y = C\Delta x + D\left(\Delta u_{new} + \Delta w\right) \tag{25}$$

Therefore, after rearranging equations (22-25), the augmented system matrix can be written as:

$$A_{aug} = \begin{bmatrix} A - BK_x & \vdots & -BK_y \\ \cdots\cdots\cdots & \vdots & \cdots\cdots \\ -\left(C - DK_x\right) & \vdots & DK_y \end{bmatrix} \text{ and } B_{aug} = \begin{bmatrix} B \\ -D \end{bmatrix} \tag{26}$$

The revised cost function for LQI controller can be defined as:

$$J_{new} = \int_0^\infty \left(\Delta x_{new}{}^T Q_{new} \Delta x_{new} + \Delta w^T R_{new} \Delta w\right) dt \tag{27}$$

The value of $K_{lqi} = R_{new}^{-1} B_{aug}^T P_{new}$ is calculated by using the Riccati equation as:

$$A_{aug}^T P_{new} + P_{new} A_{aug} - P_{new} B_{aug} R_{new}^{-1} B_{aug}^T P_{new} + Q_{new} = 0 \tag{28}$$

The values of Q_{new} and R_{new} are considered as:

$$Q_{new} = eye(10) \tag{29}$$

$$R_{new} = eye(5) \tag{30}$$

IV. Simulation Results

In this paper, the LQI control technique provides a new approach for stator and rotor active-reactive power as well as the generator-angular speed control of the DFIG system. To examine the effectiveness of the proposed control technique, the eigenvalues and step response analysis have been used. The simulation studies of the studied system have been carried out at 10% (i.e. 0.1 pu) reduction in the mechanical torque for t=0 to 25 seconds through MATLAB/SIMULINK software in the three different cases:

(a) without controller (b) LQR controller and (c) LQI controller.

The simulation results provide the LQR and LQI controller gain parameters such as K_{lqr} (5×5) which represent the optimal state feedback gain matrix, K_x (5×5) represent the proportional gain matrix and K_y (5×5) is the integral gain matrix as follows:

$$K_{lqr} = \begin{bmatrix} -2.157 & 2.445 & -3.156 & 2.420 & -0.739 \\ -2.440 & -2.142 & -2.416 & -3.140 & -3.267 \\ -3.147 & -2.420 & -2.160 & -2.456 & -0.652 \\ 2.417 & -3.157 & 2.453 & -2.169 & -1.093 \\ 0.018 & 0.056 & 0.018 & 0.056 & 3.772 \end{bmatrix}$$

$$K_x = \begin{bmatrix} -2.161 & 2.455 & -3.160 & 2.430 & -0.599 \\ -2.445 & -2.153 & -2.421 & -3.151 & -3.335 \\ -3.154 & -2.417 & -2.166 & -2.453 & -0.503 \\ 2.405 & -3.164 & 2.442 & -2.176 & -0.916 \\ 0.015 & 0.058 & 0.015 & 0.058 & 4.121 \end{bmatrix}$$

$$K_y = \begin{bmatrix} -0.549 & -0.544 & 0.565 & -0.280 & 0.067 \\ 0.573 & 0.045 & 0.258 & -0.742 & -0.228 \\ 0.005 & -0.572 & -0.731 & -0.335 & 0.159 \\ 0.606 & -0.555 & 0.264 & 0.469 & 0.185 \\ -0.058 & -0.256 & -0.094 & 0.196 & -0.940 \end{bmatrix}$$

The system matrices of the linearized model are obtained in all the cases to find out the eigenvalues, damping ratios and the damped frequencies of the studied system, which are listed in Table I. The negative real part of the eigenvalues in Table I confirms the studied system is stable in all the three different cases. In particular, the complex conjugate eigenvalues are present in all the cases which lead to the DFIG system in an oscillatory mode, whereas the real eigenvalues describe a non-oscillatory mode. From Table I, it is also seen that the real and imaginary part of all the eigenvalues in the case of the LQR and LQI controller have more negative and lower values than the case of without controller. Therefore, stability and robustness of the studied system have been significantly improved in both the LQR and LQI control techniques.

TABLE 1 EIGENVALUES ANALYSIS OF THE STUDIED SYSTEM

Without Controller (Damped Frequency, Damping Ratio)	LQR Controller (Damped Frequency, Damping Ratio)	LQI Controller (Damped Frequency, Damping Ratio)
$-16.18 \pm j313.51$ (49.90 Hz, 5.15 %)	$-6261.88 \pm j110.50$ (17.59 Hz, 99.98%)	$-6261.88 \pm j110.50$ (17.59 Hz, 99.98 %)
$-14.49 \pm j120.07$ (19.11 Hz, 11.96 %)	$-208.23 \pm j109.36$ (17.41 Hz, 88.53 %)	$-208.23 \pm j109.36$ (17.41 Hz, 88.53 %)
−4.90 (0 Hz, 100%)	−4.17 (0 Hz, 100%)	−4.17 (0 Hz, 100%)
-	-	−1.31 (0 Hz, 100%)
-	-	−1.14 (0 Hz, 100%)
-	-	−0.42 (0 Hz, 100%)
-	-	−0.32 (0 Hz, 100%)
-	-	−0.23 (0 Hz, 100%)

A. Comparative Analysis of the LQR and LQI controllers

As can be seen in Table I, only one real eigenvalue is present in the LQR controller case, while six real eigenvalues are present in the LQI controller case. This shows that stability of the studied system is improved in the LQI controller case. These two controllers are also compared with the help of dynamic responses of the output powers as well as in the generator-angular speed of the studied system. The different step responses are shown in Figs 4-8, in which the blue dotted and green solid lines represent the responses for the LQR and LQI controller, respectively.

As seen from Figs. 4-8, the deviations in the electrical powers and the generator-angular speed, are come back to zero after some time in the LQI controller case. This is because of the fact that the LQR controller without integral control yields very large steady-state offset values. However, in the proposed controller, the integral action enforces the complete rejection of any disturbances introduced in the control loop. Thus, it can be concluded that the LQI controller provides robust performance for disturbance rejection in case of the mechanical torque disturbance.

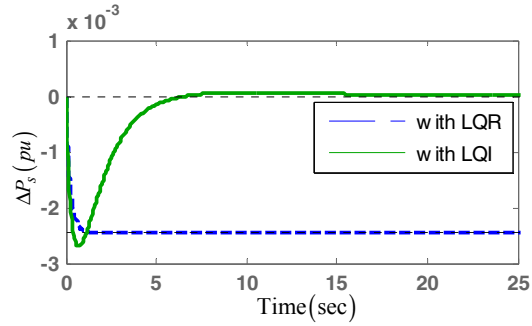

Fig.4: Step response of ΔP_s at 10% decrease in mechanical torque

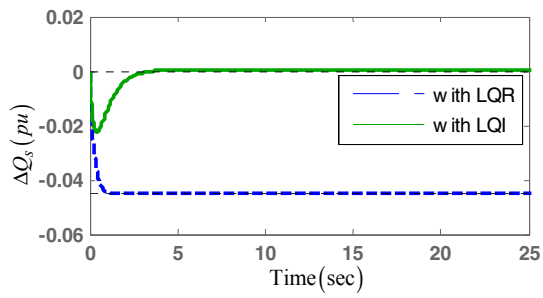

Fig.5: Step response of ΔQ_s at 10% decrease in mechanical torque

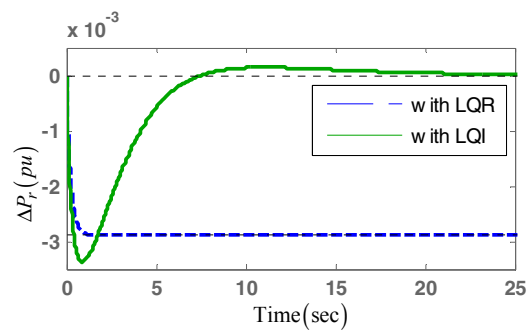

Fig.6: Step response of ΔP_r at 10% decrease in mechanical torque

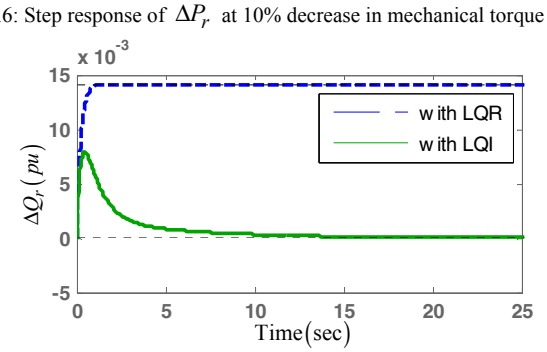

Fig.7: Step response of ΔQ_r at 10% decrease in mechanical torque

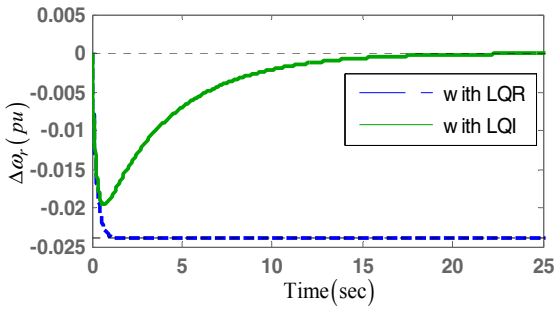

Fig.8: Step response of $\Delta\omega_r$ at 10% decrease in mechanical torque

V. Conclusions

To design the proposed controller, first, the studied system has been described by the state-space linearization methodology and then small-signal stability analysis of the study system has been done using LQR and LQI controller on the basis of eigenvalues and the dynamic responses obtained.

From the results, it can be observed that the small-signal stability and the robustness of the studied system are greatly enhanced in the LQI controller case. Therefore, LQI controller is more suitable to utilize to control the DFIG angular speed and power flows through the DFIG.

References

[1] G. Abad, J. Lopez, M. Rodríguez, L. Marroyo, and G. Iwanski, "Doubly fed induction machine: modeling and control for wind energy generation," *IEEE Press Ser. power Eng.*, 2011.

[2] H.-S. Ko, J. Jatskevich, G. Dumont, and G.-G. Yoon, "An advanced LMI-based-LQR design for voltage control of grid-connected wind farm," *Electr. Power Syst. Res.*, vol. 78, no. 4, pp. 539–546, 2008.

[3] J. X. Ostolaza, A. Etxeberria, and I. Zubia, "Wind farm node connected DFIG / back-to-back converter coupling transient model for grid integration studies," *Energy Convers. Manag.*, vol. 106, pp. 428–439, 2015.

[4] L. Xu and Y. Wang, "Dynamic modeling and control of DFIG-based wind turbines under unbalanced network conditions," *IEEE Trans. Power Syst.*, vol. 22, no. 1, pp. 314–323, 2007.

[5] Y. Lei, A. Mullane, G. Lightbody, and R. Yacamini, "Modeling of the Wind Turbine With a Doubly Fed Induction Generator for Grid Integration Studies," *IEEE Trans. Energy Convers.*, vol. 21, no. 1, pp. 257–264, 2006.

[6] F. Mei and B. Pal, "Modal analysis of grid-connected doubly fed induction generators," *IEEE Trans. Energy Convers.*, vol. 22, no. 3, pp. 728–736, 2007.

[7] F. Mei and B. C. Pal, "Modelling and small-signal analysis of a grid connected doubly-fed induction generator," in *2005 IEEE Power Engineering Society General Meeting*, 2005, vol. 3, pp. 2101–2108.

[8] B. C. Pal and F. Mei, "Modelling adequacy of the doubly fed induction generator for small-signal stability studies in power systems," *IET Renew. Power Gener.*, vol. 2, no. 3, p. 181, 2008.

[9] P. Kundur, *Power System Control and Stability*. New York: Mcgraw-Hill, Inc., 1994.

[10] B. Mehta, P. Bhatt, and V. Pandya, "Small signal stability analysis of power systems with DFIG based wind power penetration," *Int. J. Electr. Power Energy Syst.*, vol. 58, pp. 64–74, 2014.

[11] Y. Zhang, D. Xie, J. Feng, and R. Wang, "Small-signal Modeling and Modal Analysis of Wind Turbine Based on Three-mass Shaft Model," *Electr. Power Components Syst.*, vol. 42, no. March 2015, pp. 693–702, 2014.

[12] Y. Mishra, S. Mishra, F. Li, Z. Y. Dong, and R. C. Bansal, "Small-signal stability analysis of a DFIG-based wind power system under different modes of operation," *IEEE Trans. Energy Convers.*, vol. 24, no. 4, pp. 972–982, 2009.

[13] H. Yuan, Y. Shang, and X. Fu, "Improved diagonal interacting multiple model algorithm for manoeuvering target tracking based on H ∞ filter," *IET Control Theory Appl.*, vol. 9, no. 12, pp. 1887–1892, 2015.

[14] A. Kalbat, "Linear Quadratic Gaussian (LQG) Control of wind turbines," *2013 3rd Int. Conf. Electr. Power Energy Convers. Syst. EPECS 2013*, vol. 0, no. 2, pp. 1–5, 2013.

[15] K. Ogata, *Modern control engineering*, 4th ed.,. Prentice Hall, Aeeizh, 2002.

[16] J. M. Macijejowski, *Multivariable Feedback Design*, 1st ed. Addison-Wesley, Cornwall, Great Britain, 1989.

[17] Fodor A., M. A., and H. K. M., "Multiple-Input–Multiple-Output Linear-Quadratic Control of the Energy Production of a Synchronous Generator in a Nuclear Power Plant," *Electr. Power Components Syst.*, vol. 42, no. 15, pp. 1673–1682, 2014.

[18] C. Verde, J. L. Rojas A., and C. R. Fuerte-Esquivel, "Improving Stability Margin in Electric Power Systems by Linear Quadratic Regulator and Disturbance Model," *Electr. Power Components Syst.*, vol. 41, no. 14, pp. 1415–1431, 2013.

[19] P. C. Young and J. C. Willems, "An approach to the linear multivariable servomechanism problem.," *Int. J. Control*, vol. 15, no. 5, pp. 961–979, 1972.

[20] R. Bhushan, K. Chatterjee, and R. Shankar, "Comparison between GA-based LQR and Conventional LQR Control Method ofDFIG Wind Energy System," in *Recent Advances in Information Technology (RAIT), 2016 3rd International Conference, Dhanbad, India*, 2016.

[21] S. Das, I. Pan, K. Halder, S. Das, and A. Gupta, "LQR based improved discrete PID controller design via optimum selection of weighting matrices using fractional order integral performance index," *Appl. Math. Model.*, vol. 37, pp. 4253–4268, 2013.

[22] S. Srivastaval and V. S. Pandit, "A Scheme to Control the Speed of a DC Motor with Time Delay using

LQR-PID controller," in *IEEE, International Conference on Industrial Instrumentation and Control (ICIC), India*, 2015.

[23] S. Carriere, S. Caux, and M. Fadel, "Optimal LQI Synthesis for Speed Control of Synchronous Actuator under Load Inertia Variations," *Int. Fed. Autom. Control Seoul, Korea*, pp. 5831–5836, 2008.

[24] M. Ge, M.-S. Chiu, and Q.-G. Wang, "Robust PID controller design via LMI approach," *J. Process Control*, vol. 12, no. 1, pp. 3–13, 2002.